

AD-A066 820

FOREIGN TECHNOLOGY DIV WRIGHT-PATTERSON AFB OHIO
CALCULATION OF THE EFFECTIVE ARMATURE CURRENT LOAD OF THE SYNCH--ETC(U)
APR 78 J STEPINA

F/G 9/3

UNCLASSIFIED

FTD-ID(RS)T-0392-78

NL

| OF |
AD
A066820



AD-A066820

1

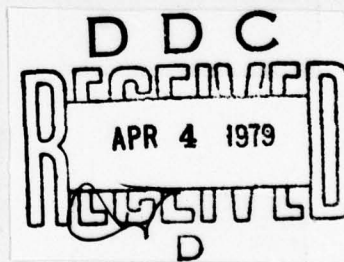
FOREIGN TECHNOLOGY DIVISION



CALCULATION OF THE EFFECTIVE ARMATURE CURRENT
LOAD OF THE SYNCHRONOUS MACHINE
UNDER RECTIFIER LOAD

by

Jaroslav Stepina



Approved for public release;
distribution unlimited.

78 09 08 075

ACCESSION NO.	
DTIC	White Section <input checked="" type="checkbox"/>
DDI	Grey Section <input type="checkbox"/>
UNANNOUNCED	<input type="checkbox"/>
JUSTIFICATION	
BY	
DISTRIBUTION/AVAILABILITY ROOMS	
Dist.	AVAIL. and/or SPECIAL
A	

FTD-ID(RS)T-0392-78

EDITED TRANSLATION

FTD-ID(RS)T-0392-78

3 April 1978

MICROFICHE NR: *FTD-78-C-000474*

CALCULATION OF THE EFFECTIVE ARMATURE CURRENT LOAD
OF THE SYNCHRONOUS MACHINE UNDER RECTIFIER LOAD

By: Jaroslav Stepina

English pages: 32

Source: Acta Technica CSAV, No. 3, 1964, pp. 255-280

Country of origin: Czechoslovakia

Translated by: LINGUISTICS

F33657-76-D-0389

Chester E. Claff, Jr.

Requester: AFAPL/POD

Approved for release; distribution unlimited.

THIS TRANSLATION IS A RENDITION OF THE ORIGINAL FOREIGN TEXT WITHOUT ANY ANALYTICAL OR EDITORIAL COMMENT. STATEMENTS OR THEORIES ADVOCATED OR IMPLIED ARE THOSE OF THE SOURCE AND DO NOT NECESSARILY REFLECT THE POSITION OR OPINION OF THE FOREIGN TECHNOLOGY DIVISION.

PREPARED BY:

TRANSLATION DIVISION
FOREIGN TECHNOLOGY DIVISION
WP-AFB, OHIO.

FTD-ID(RS)T-0392-78

Date 3 April 1978

78 09 08 075

Calculation of the ^EAffective Armature Current Load of the Synchronous Machine Under Rectifier Load

Jaroslav Stepina

1. INTRODUCTION

Rectifiers are constantly increasing in importance in high-voltage current technology, and recently have been replacing other types of direct current sources. With the regulated rectifier, the synchronous machine forms an independent source of direct current, which can be used, for example, as an exciter of the large synchronous alternator. The rectifier load is very unfavorable for the synchronous machine, which supplies the rectifier, because it is a matter of non-sinusoidal pulse-shaped currents with which the machine is loaded. Significant additional losses occur both in the stator as well as in the rotor, which must be considered in the design of the machine. In particular, the additional losses in the rotor are frequently determining for the choice of the rated output of the generator and must be carefully determined. This additional loss is ordinarily calculated based on the harmonic^s analysis of the armature currents (1). Each solitary wave of the armature current corresponds to a series of additional fields in the air gap, which bring about currents in the damping winding, exciter coil, and in the iron, and in this way cause additional losses. In this calculation method, the losses are calculated independently for each solitary wave of the armature current, whereby the possibility occurs of taking into consideration the increase of the armature imped^aence with the frequency of the induced current. However, if we wish to compare the various circuits from the standpoint of the additional losses, this process is rather laborious, since we must first resolve the armature current into component waves, determine their effect on the armature, and then total the individual component losses. In this way, we also lose^e the concept of the distribution of these losses at the armature periphery, which tends not to be uniform.

In the present paper is shown a simple calculation method for the additional current load of the armature, which is particularly suitable for the preliminary comparison of various circuits, and which also facilitates the calculation in complicated cases with consideration of the commutation processes.

* We initially show a direct calculation of the effective current load of the damping winding in a simple example of a three-phase rectifier which is supplied from a three-phase turbo-generator (Figure 1). We assume that the direct current I_g is completely smoothed out by the large inductance of the direct current circuit, so that it contains no harmonic currents, and we ignore for the moment the overlap of the power supply of the commutating rectifiers brought about by the inductance of the generator winding. With

*2. The effective current load of the Armature

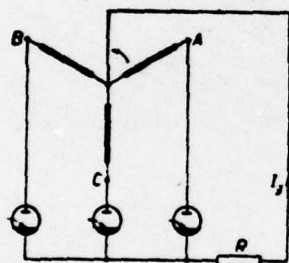


Figure 1

Synchronous machine with rectifier load

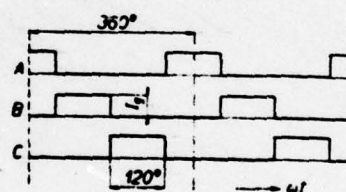


Figure 2

Shape of the line currents

this assumption, the currents in individual rectifiers and winding lines are shaped as shown in Figure 2. Each anode conducts the entire current during the period corresponding to one-third of the current period. The other two winding lines at this time have no current flow. Let us now consider how the fundamental wave of the stator current load travels. It is apparent from Figures 1 and 2 that this wave is at rest during the period of conduction of a line towards the

stator, and then suddenly changes its position by 120° (in the two-pole machine). If we visualize this current wave as a vector $i_{(1)}$ in the coordinate system connected with the rotors, we obtain the spatial motion of this vector with time as illustrated in Figure 3. During the time of current conductance of an anode, the vector $i_{(1)}$ moves towards the rotor with the angular velocity of the rotor, and after rotating by an angle of 120° , it jumps forward by the angle of 120° . The end point of the vector $i_{(1)}$, therefore, circumscribes the arc between the limiting vectors $(i_{(1)})'$ and $(i_{(1)})''$. It is apparent from this in what way the rectifier load differs from the standard. In the rectifier load of the generator, the armature reaction moves forward in jumps, whereas in a normal load it rotates uniformly with the armature. The number of jumps corresponding to one rotation is given here by the number of anodes m , generally by the number of pulses m'' , i.e., by the number of successive ignitions per period of the alternating current. We will now show that the alternating current load of the armature can be determined by analysis of the motion of the vector $i_{(1)}$ in the Gaussian complex plane (Figure 3) connected with the armature. The vector $i_{(1)}$ which describes an arc between the limiting positions $(i_{(1)})'$ and $(i_{(1)})''$ periodically in the Gaussian complex plane of the armature coordinates, is a periodic complex function which can be ~~developed~~^{expanded} in series

$$(1) \quad i_{(1)} = \sum_{n=-\infty}^{n=+\infty} I_{(1)n} e^{jn\pi x}$$

where n represents whole positive and negative numbers including zero. The variable x in our case depends on the time and changes by 2π for each period of the complex function. For the individual terms of this series, the following equation applies:

$$(2) \quad I_{(1)n} = \frac{1}{2\pi} \int_0^{2\pi} i_{(1)} e^{-jn\pi x} dx.$$

This development represents a resolution of the periodic complex function into a series of component vectors which, however, rotate at various velocities in the positive (for positive n) or negative

(for negative n) direction. One of these vectors will also have zero angular velocity, and it is obtained from the Equation (2) for $n = 0$

$$(3) \quad I_{(1)0} = \frac{1}{2\pi} \int_0^{2\pi} i_{(1)} dx.$$

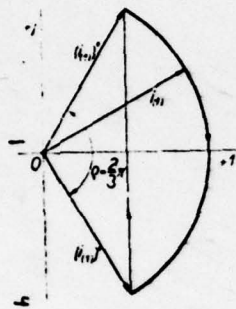


Figure 3. Space vector of the fundamental wave of the air gap field.

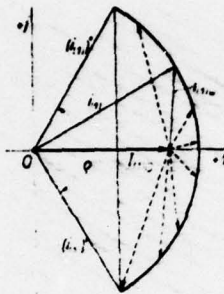


Figure 4. Resolution of the space vector.

The vector $I_{(1)0}$ represents the average value of the periodically variable vector $i_{(1)}$ in question, i.e., in our case it represents the components of this vector which retain their values unchanged and which rotate synchronously with the armature (see Figure 4). We can convince ourselves that this vector corresponds to the fundamental wave of the stator current, and that we can obtain it also based on the resolution of the stator current into component waves. The other components determined by Equation (2) for $n \neq 0$ represent circular fields which also retain their values unchanged, but which move towards the armature with different angular velocities. The fundamental velocity corresponds to a single rotation per period of the analyzed vector (change of x by 2π). Because m'' period^s of the vector under consideration, i.e., three periods in our case, correspond to one period of the rotor current, where $m'' = 3$ is

the number of pulses, the angular velocity of the component field is given by Equation (4)

$$(4) \quad \omega_n = nm^* \omega_m = 3n\omega_m$$

where ω_m signifies the velocity of the armature and n is the ordinal number from Equations (1) and (2)¹⁾. (Footnote on page 6)

If we were to resolve the rotor currents into component waves, we would convince ourselves that each component $I_{(1)n}$ of the vector $I_{(1)}$ of the n^{th} order corresponds to a specific component wave of the stator current with the order number

$$(5) \quad v = |3n + 1|,$$

where $n = \pm 1, \pm 2, \pm 3, \dots$. It is apparent from this, that by the resolution of the periodically variable vector we obtain directly the fields which correspond to the component waves of the stator current, which bring about the fundamental wave of the air gap field. The integrations in the exponential form of Equation (2), however, are simpler than by the customary Fourier development, so that this method of calculation can be used particularly in the complicated cases with consideration of the overlapping. However, it is not a question only of obtaining the components of the air gap field or of the current load in another way without resolution of the stator currents, but of the calculation without any ~~development~~^{expansion} in series. If, in the informative calculation, we ignore the fact that for higher frequencies, the rotor resistance is greater, because of the current displacement, then for the strongest component wave (here 150 Hz) of the rotor current, the momentary value of the rotor losses is determined by the square of the alternating current components of the vector $i_{(1)}$, i.e., by the value

$$(6) \quad |i_{(1)w}|^2 = i_{(1)w}^2 = |i_{(1)} - i_{(1)0}|^2$$

since the component $I_{(1)0}$ rotates with the rotor and causes no damping current in the rotor (see Figure 4). The effective value of the component $i_{(1)w}$ is found to be

$$(7) \quad I_{(1)w} = \sqrt{\left(\frac{1}{2\pi} \int_0^{2\pi} i_{(1)w}^2 dx\right)}.$$

If we consider that for $|n_1| \neq |n_2|$

$$(8) \quad \begin{aligned} \int_0^{2\pi} \sin n_1 x \sin n_2 x dx &= \int_0^{2\pi} \cos n_1 x \cos n_2 x dx = \\ &= \int_0^{2\pi} \sin n_1 x \cos n_2 x dx = 0 \end{aligned}$$

and for $n_1 = -n_2$

$$(8a) \quad \int_0^{2\pi} \cos n_1 x \cos n_2 x dx = - \int_0^{2\pi} \sin n_1 x \sin n_2 x dx$$

from equations (1), (6) and (7), we can write

$$(9) \quad I_{(1)w} = \sqrt{\left(\frac{1}{2\pi} \int_0^{2\pi} |i_{(1)}|^2 dx - |i_{(1)0}|^2\right)} = \sqrt{(I_{(1)}^2 - I_{(1)0}^2)},$$

where

$$(10) \quad I_{(1)} = \sqrt{\left(\frac{1}{2\pi} \int_0^{2\pi} |i_{(1)}|^2 dx\right)}$$

represents the effective value of the entire current wave $i_{(1)}$, and $I_{(1)0}$ is given by Equation (3).

The value $I_{(1)w}$ represents the amplitude of the equivalent circuit field (better stated, of the equivalent circuit current load), which would bring about the same losses in the armature

1) The resolution of the periodically variable vector based on the indicated procedure into a rest component and a series of rotational components, include also the usual resolution of the pulsating field into two circular fields. (Footnote for page 5)

as the current wave illustrated by the vector, if the increase of the effective impedance of the armature were not to come into play at higher frequencies. We are particularly interested in the ratio of the value $I_{(1)w}$ to the working wave $I_{(1)0}$, i.e., in accordance with (9) for

$$(11) \quad A_{(1)} = \frac{I_{(1)w}}{I_{(1)0}} = \sqrt{\left(\frac{I_{(1)}^2}{I_{(1)0}^2} - 1\right)}.$$

The value $A_{(1)}$ represents the relative value of the circular field which, as far as the heat effects are concerned, replaces the effect of the stator current wave of order $(v) = 1$ on the armature. There is also available here the comparison with the counteracting components in the unsymmetrical load, whose permissible value is known from experience, and is stated to be 10% for turbo-generators and 20% for hydrogenerators. A definite difference consists only of the fact that the counteracting component loads the periphery of the rotor uniformly with the currents of equal frequency (generally 100 Hz), whereas the value $A_{(1)}$ represents a spatially sinusoidal but temporally non-sinusoidal rotor load with the fundamental frequency $f_1 = m \cdot f$. In our case of a three-phase rectifier, this fundamental frequency is $f_1 = 150$ Hz. In an exact calculation, it is necessary to take this difference into account.

In our case of a three-phase circuit, we obtain from Equation (3)

$$(12) \quad I_{(1)0} = \frac{1}{2\pi} \int_0^{2\pi} i_{(1)} dx = \frac{1}{2\pi} \int_0^{2\pi} |i_{(1)}| e^{-j(x/3 - \pi/3)} dx = \frac{3\sqrt{3}}{2\pi} I_{(1)m} = 0,827 I_{(1)m}$$

and further from (10)

$$(13) \quad I_{(1)} = |i_{(1)}| = I_{(1)m},$$

so that according to (11)

$$(14) \quad A_{(1)} = \frac{I_{(1)w}}{I_{(1)0}} = \sqrt{\left[\left(\frac{2\pi}{3\sqrt{3}}\right)^2 - 1\right]} = 0,68.$$

From the result it follows that the rectifier load in the rotor brings about additional losses which correspond to the counteracting component of 68%, which is a multiple of the usually permissible value.

In the preceding calculation, on the one hand we ignored the overlapping of the current conductance of the commutating anodes, and on the other hand, the increase of the rotor resistance with frequency, which results in a definite increase of losses. How these factors can be considered in the exact calculation is shown further below.

Let us now consider how the individual components participate in the losses determined by the value $\hat{A}_{(1)}$. From Equation (2), it follows that

$$(15) \quad I_{(1)n} = \frac{1}{2\pi} \int_0^{2\pi} I_{(1)} e^{-jnx} dx = \frac{1}{2\pi} I_{(1)m} \int_0^{2\pi} e^{-j(x/3 - \pi/3)} e^{-jnx} dx = \\ = I_{(1)m} \frac{3\sqrt{3}}{2\pi} \frac{1}{3n+1}.$$

Since the order number ν of the associated component wave of the stator current appears in the denominator of Equation (15) (see Equation (5)), the strongest components from Equation (15) correspond to the second and fourth harmonics of the stator current. The relative value of the equivalent circuit field for these two waves is given in accordance with (12) and (15), by

$$(16) \quad A_{1-1} = \frac{\sqrt{(|I_{(1)2}|^2 + |I_{(1)4}|^2)}}{I_{(1)0}} = \sqrt{\left[(-\frac{1}{2})^2 + (\frac{1}{4})^2\right]} = \sqrt{\frac{5}{16}} = 0,56.$$

It results from Equation (16), that of the total value of 68%, which represents the effect of all the waves, the two strongest waves, which induce the frequency of 150 Hz in the rotor, make up 56%, so that their influence predominates.

3. Various Rectifier Circuits

It was shown in Section 2, how the additional losses in the rotor of the synchronous machine loaded with a rectifier in three-

phase circuit, caused by the fundamental wave of the current load, can be simply estimated. In practice, however, complicated circuits are used, which are to be found in the ordinary literature (4, 8, 9). Some characteristic circuits are shown in Tables I and II. Table I contains the center-tapped circuits, and Table II characteristic bridge circuits. In columns a), b), c), the diagrams of windings and rectifier circuits are indicated; in columns d), e), f), the shapes of the current flows with the associated values of the ratio I/I_1 of the effective value of the total current to the effective value of the fundamental wave are illustrated. The values of I/I_1 are determining for the use of the conductor material of the associated winding. The diagrams also contain the transformer, so that the "circuit currents" listed for the generator load are determining, when the rectifier is fed by the generator not directly but through a transformer. When the transformer is not present, and the rectifier is fed directly, the current shape corresponding to the secondary winding of the transformer applies to the generator. In column g), the number $\frac{m}{\pi}$ of successive commutations per period of the generator voltage, i.e., the number of pulses of the direct current side, are indicated. Other columns are connected with the analysis of the electromagnetic processes in the generator listed here. The angle ϱ (column h) is the angle limiting the oscillation of the fundamental wave of the armature reaction around the average value based on the rotor (see Figures 4 and 3). If we follow the current in a single winding line, we determine that the angle ϱ does not depend on whether the rectifier is connected to the generator directly or through a transformer. It is indeed true, that in the use of the transformer between the rectifier and generator, certain current harmonics

1) The difference between d) and e) corresponds to the direct current component or to the harmonics of even order.

2) The difference between e) and f) corresponds to the harmonics of the order $\nu = 3k$ (delta-connection).

Table 1. Center-tap Circuits

		1	2	3
a)	Primärwicklung			
b)	Sekundärwicklung			
c)	Ventil			
d)	Sekundärstrom	1.48	1.82	1.48
e)	Primärstrom	1.21	1.28	1.05
f)	Netzstrom	1.21	1.05	1.05
g)	m	3	6	6
h)	φ	$\frac{2}{3}\pi$	$\frac{\pi}{3}$	$\frac{\pi}{3}$
i)	i_{mo}/i_{sum}	0.827	0.955	0.955
j)	$\Lambda_{1,11}$	0.68	0.311	0.311
k)	ν_0	-2.4	-5.7	-5.7
l)	$\Lambda_{1,1}$	0.55	0.25	0.25
m)	f_1	150	300	300
n)	$S_{(M)}$	$2N\dot{s}_{(M)}$	$2N\dot{s}_{(M)}$	$2N\dot{s}_{(M)}\cos(\pi/6)$

a) Primary winding

b) Secondary winding

c) Rectifier

d) Secondary current

e) Primary current

f) Circuit current

(Explanation 1) and 2) on page 9.)

(e.g. the third and harmonics of even order or the direct current component) disappear, but there are such harmonics which do not participate in the generation of the fundamental wave of the field in the air gap, so that the fundamental wave of the armature reaction is not affected by the transformer. The angle φ listed in column h), therefore, applies both to the direct and the indirect supply through a transformer.

One might believe that the pursuit of the space motion of the vector $i_{(1)}$ in the circuits with two parallel systems must be tedious (see for example, Diagram 4 in Table II), but the space

vector can be studied as the sum of two component vectors of the two parallel systems. For example, in the circuit 4 in Table II, the component vector of each parallel system changes its position by 60° , so that the resulting vector always jumps by the angle $\varrho = \frac{1}{2} \cdot 60^\circ = 30^\circ$. It is apparent that for the angle ϱ ,

$$\varrho = \frac{2\pi}{m''} \quad (17)$$

Table II. Bridge Circuits

		1	2	3	4
a)	Primärwicklung				
b)	Sekundärwicklung				
c)	Ventil				
d)	Ventilstrom				
e)	Primärstrom Sekundärstrom				
f)	Netzstrom				
g)	m'	6	6	6	12
h)	φ	$\frac{\pi}{3}$	$\frac{\pi}{3}$	$\frac{\pi}{3}$	$\frac{\pi}{6}$
i)	$\frac{I_{m1}}{I_{m2}}$	0.955	0.955	0.955	0.989
j)	Λ_{m1}	0.311	0.311	0.311	0.153
k)	φ	-5.7°	-5.7°	-5.7°	-11.1°
l)	Λ_{m2}	0.25	0.25	0.25	0.12
m)	I_1	300	300	300	600
n)	S_m	$4N \frac{1}{2} \cos \frac{\pi}{6}$	$\frac{4}{3} N \frac{1}{2} \cos \frac{\pi}{3}$	$2N \frac{1}{2} \cos \frac{\pi}{3}$	$\frac{1}{2} S_m \cos \frac{\pi}{6}$

- a) Primary winding
b) Secondary winding
c) Rectifier
d) Rectifier current

- e) Primary current
f) Secondary current
g) Circuit current

1) The difference between e) and f) corresponds to the harmonics of order $\nu = 3k$ (delta circuit).

2) The difference between e) and f) corresponds to the harmonics of order $\nu = 5, 7, 17, 19$, etc.

In column i) of Tables I and II are the average values $I_{(1)0}$ of the vector $i_{(i)}$, which can be calculated for any desired angle α in accordance with Equation (3). The following Equation applies:

$$(18) \quad I_{(1)0} = \frac{1}{2\pi} \int_0^{2\pi} I_{(1)} dx = \frac{1}{2\pi} I_{(1)m} \int_0^{2\pi} e^{-j(x/m'' - \pi/m'')} dx = I_{(1)m} \frac{m''}{\pi} \sin \frac{\pi}{m''}$$

and for the relative size of the equivalent circuit field, according to Equation (11), we obtain

$$(19) \quad A_{(1)} = \frac{I_{(1)m}}{I_{(1)0}} = \sqrt{\left[\frac{I_{(1)}^2}{I_{(1)0}^2} - 1 \right]} = \sqrt{\left[\left(\frac{\pi}{m'' \sin \pi/m''} \right)^2 - 1 \right]},$$

which is a generalization of Equation (14). The values of $A_{(1)}$ are listed for each circuit in column j of Tables I and II. It follows from the values of $A_{(1)}$, that the rotor load declines rapidly with the number of ignitions per period, i.e., with the number of pulses m'' . In this decline of the effective load, the current harmonics of lowest order disappear stepwise, so that in the circuits with large m'' , a rather large increase of the rotor resistance is to be expected, which results from the current dislocation. We represent this better if we ~~develop~~^{expand} the vector $i_{(i)}$ in series ~~from~~^{to} circular fields. For the n^{th} component of the vector $i_{(i)}$, we obtain from

$$(20) \quad I_{(1)n} = \frac{1}{2\pi} \int_0^{2\pi} I_{(1)} e^{-jn\alpha} dx = \frac{1}{2\pi} I_{(1)m} \int_0^{2\pi} e^{-j(x/m'' - \pi/m'')} e^{-jn\alpha} dx = \\ = I_{(1)m} \frac{m''}{\pi(m''n + 1)} \sin \frac{\pi}{m''}.$$

From Equation (20), we obtain for $n = 0$, the average value

$$(21) \quad I_{(1)0} = I_{(1)m} \frac{m''}{\pi} \sin \frac{\pi}{m''}$$

and the ratio

$$(22) \quad \frac{I_{(1)n}}{I_{(1)0}} = \frac{1}{m''n + 1}.$$

Equations (20) to (22) show us a number of interesting relationships. If we expand the shape of the stator current into a series and compare the results with Equation (22), we determine that the denominator in Equation (22) represents in its size the order number of that stator current wave which produces the associated component $I_{(1)n}$. Therefore, we can state as a generalization of Equation (5)

$$(23) \quad v = |m''n + 1|$$

and by substitution in Equation (22), we obtain

$$(24) \quad \frac{I_{(1)n}}{I_{(1)0}} = \frac{1}{v}.$$

It is demonstrated in general by Equation (24), that if the commutation is not taken into consideration, the type of circuit does not ^affect the relative values of the current harmonics which the fundamental wave of the air-gap field produces. These current harmonics, which participate in the fundamental wave of the air-gap field, and the associated field components, decline in accordance with (24) with the order number v , and they cannot be excluded by insertion of any desired transformer between the rectifier and the generator. Only the number of pulses m'' is determining for their appearance. If a complicated circuit with a large number of pulses is used, certain component waves are indeed excluded in accordance with (23), but the remainder are not influenced. The larger the number of pulses m'' , then the more terms disappear in the series of order numbers v , and the series then begins at higher values of v . The reduction of the value of $I_{(1)}$ with the increasing number of pulses m'' can therefore be attributed to the stepwise degeneration of harmonics of the lowest order. The harmonics whose order is given by Equation (23), therefore, form a minimum harmonics content of the stator current. The

harmonics which are suppressed by the bridge circuit or in the transformer, corresponds to the air gap fields of higher order (N), as will be shown later.

In Tables I and II, in column k , are listed the orders ν_0 of the strongest components (for $n = \pm 1$), and in column 1 are listed the relative rotor current loads caused by these components

$$(25) \quad A_{1-1} = \frac{\sqrt{[I_{(00)}]^2 + [I_{(0-1)}]^2}}{|I_{(10)}|}.$$

The frequency of the currents caused by these components ($n = \pm 1$) in the rotor is $f_1 = m''f$, where f is the frequency of the alternating voltage of the stator. It is apparent from this, that it is true in general that the fundamental wave of the alternating component of the direct current and the strongest component of the current in the damping winding have the same frequency. Therefore, the additional rotor losses of the generator can be judged according to the pulsed frequency of the direct current voltage. That is to say, it does not depend on the number of rectifiers but on the number of successive commutations, i.e., on the number of pulses, which is smaller than the number of rectifiers in the simultaneous commutation of two or more rectifiers. For example, circuit 3 in Table II has 12 rectifiers, but it shows the same properties as the circuits with 6 rectifiers. Because of this, from the standpoint of rotor losses, there is no advantage to those circuits in which two or more rectifiers commute simultaneously. From the standpoint of the generator, circuits 3 in Table I and 2 and 3 in Table 2 are equivalent. The bridge circuits have the advantage of a more simple supply of the three-phase winding, which is balanced against the drawback that the overall current I_g flows through two rectifiers connected in series. In the direct supply (without transformer) of the rectifier by the generator, it is advantageous that the harmonics content of the current be limited by the bridge circuit itself to the unavoidable minimum. Of all the circuits listed in Tables I and II, the smallest losses are shown by circuit 4 in Table II, with 12 rectifiers which commute successively.

4. Harmonics of the Stator Current Distribution

In the previous considerations, we took into consideration only the fundamental wave of the rotor current distribution, and it still remains to discuss the effect of the harmonics. The harmonics of the stator current distribution form with the rotor a series of asynchronous machines with a larger number of poles than the machine actually has. These waves produce reactions of the rotor similar to the fundamental wave reactions, and are damped by the rotor. For the calculation of their effect, we can use the same procedure as for the fundamental waves. We can again visualize these current waves as vectors, but not directly in the space of the machine (as for the fundamental wave of a two-pole machine), but in the "electrical space" of the harmonic being considered, i.e., in the complex Gaussian plane, where the solid angle is enlarged (ν) times. The size of the vector of the chosen harmonic of the current distribution can be expressed by the equation

$$(26) \quad I_{(\nu)m} = \frac{1}{\pi} S_{(\nu)} I_g$$

(see (7)), where $S_{(\nu)}$ is the effective base number for the ν^{th} harmonic based on the entire direct current flow. For example, if the rectifier in the center-tapped circuit 1 or 2 (Table I) is supplied directly from the generator (the stator winding of the generator instead of the secondary winding of the transformer) the current flows through a line and

$$(27) \quad S_{(\nu)} = 2N\xi_{(\nu)},$$

where N is the number of turns of a line, and $\xi_{(\nu)}$ is the winding factor for the ν^{th} harmonic. For the other circuits listed in Tables I and II, the formulas for $S_{(\nu)}$ are in column n). However, they apply only for the case of direct feed from the generator.

Let us now consider what shape the vector $i_{(\nu)}$ will have, which represents the ν^{th} harmonic of the current distribution in its complex Gaussian plane. It is, of course, necessary here, on the one hand, to consider those circuits in which the number of lines in the generator m_G agrees with the number of pulses of the

direct current voltage (the center-tapped circuits and certain bridge circuits) and on the other hand, the circuits in which $m_G < m''$ (the bridge circuits and the center-tapped circuits powered through a transformer).

a) Circuits with $m_G = m''$

Of the circuits shown in the tables, all circuits in Table I and circuit 3 in Table II belong to this group, if the rectifier is supplied directly from the generator (without transformer). In these circuits, it is true for each harmonic just as for the fundamental wave, that the amplitude of the component waves under consideration does not change during the period between two commutations, but that these waves move only towards the rotor as a result of its rotation with equal angular velocity. In the commutation, all component waves jump forward by the same solid angle. In the vectorial representation, all angles are enlarged (ν) -fold in the electrical space. The average value of the vector, according to the generalized Equation (18), is shown to be

$$(28) \quad I_{(\nu)0} = \frac{1}{2\pi} \int_0^{2\pi} I_{(\nu)} dx = \frac{1}{2\pi} I_{(\nu)m} \int_0^{2\pi} e^{-j((\nu)/m'')(x-\pi)} dx = \\ = I_{(\nu)m} \frac{m''}{\pi(\nu)} \sin \frac{(\nu)}{m''} \pi.$$

Just as in the case of the fundamental wave, we can also define here the relative size of the alternating component of the ν^{th} component wave, whereby they are not based on the average value of the vector concerned, but on the average value of the vector of the fundamental wave, which is the operating frequency of the machine. With this, in accordance with (28) and (26)

$$(29) \quad A_{(\nu)} = \frac{I_{(\nu)w}}{I_{(1)0}} = \frac{S_{(\nu)}}{S_{(1)}} \frac{\sqrt{\{1 - [m''/\pi(\nu)]^2 \sin^2 [(\nu)\pi/m'']\}}}{(m''/\pi) \sin (\pi/m'')} = \frac{S_{(\nu)}}{S_{(1)}} r_{(\nu)}.$$

The values of

$$(30) \quad r_{(\nu)} = \frac{\sqrt{\{1 - [m''/\pi(\nu)]^2 \sin^2 [(\nu)\pi/m'']\}}}{(m''/\pi) \sin (\pi/m'')}$$

are listed for various values of m'' and (ν) in Table III. Based on the values of $r_{(\nu)}$ listed in Table III, one would believe that the harmonics of the stator current distribution participate strongly in the rotor losses. However, it must not remain unobserved that the winding factor for the harmonics is ~~exceedingly~~ ^{exceedingly} small or even zero (for example, for the harmonics of even order). At the same time,

it must be considered in the actual calculations, that the harmonics of higher order are not completely damped out by the rotor, i.e., that the rotor current waves are smaller than the stator current waves, which generate them, since the magnetization current is comparatively large with a large number of poles, i.e., at large (ν) . In addition, in turbo generators, the most sensitive position is at the rotor end, where the current waves of higher order come into play as in the short-circuiting ring of a cage rotor, i.e., with (ν) -fold smaller values than according to Table III. In Table III, those orders which cannot be affected by insertion of a transformer between the rectifier and the generator are indicated by bold outlines. These are the harmonics which stem from the same stator current waves as the fundamental wave of the stator current distribution (see Equation (23)).

Table III Factor $r_{(\nu)}$

m° (ν)	3	6	12	24
1	0,680	0,311	0,150	0,024
2	1,102	0,588	0,300	0,148
3	1,209	0,807	0,441	0,222
4	1,183	0,954	0,568	0,298
5	1,192	1,028	0,683	0,366
6	1,209	1,047	0,715	0,437
7	1,201	1,038	0,859	0,504
8	1,202	1,024	0,921	0,564
9	1,209	1,023	0,965	0,622
10	1,204	1,032	0,998	0,677
11	1,206	1,031	1,007	0,728
12	1,209	1,047	1,011	0,773

Just as in the case of the fundamental wave, we can also expand the vector $i_{(\nu)}$ of the ν^{th} component wave into a series of circular fields according to Equation (31).

$$(31) \quad I_{(\nu)m} = \frac{1}{2\pi} \int_0^{2\pi} I_{(\nu)} e^{-jmx} dx = \frac{1}{2\pi} I_{(\nu)m} \int_0^{2\pi} e^{-j[(\nu)/m''](x-\pi)} e^{-jmx} dx = \frac{I_{(\nu)m}}{\pi} \frac{m''}{(\nu) + m''n} \sin \frac{(\nu)}{m''} \pi.$$

It can be established that in the center-tap circuits, the circular fields $I_{(\nu)n}$ correspond to the stator current harmonics according to the generalized equation (23). The following applies for the denominator of Equation (31):

$$(32) \quad \nu = (\nu) + m''n,$$

from which the negative sign on ν appears for the component waves which rotate in the opposite direction. Equation (32) can also be transformed to:

$$(33) \quad (\nu) = \nu - m''n,$$

where ν is always positive and the sign of (ν) indicates the direction of rotation.

A special case occurs when (ν) is a whole multiple of m'' . The vector $i_{(\nu)n}$ in this case will only be not equal to zero when

$$(34) \quad (\nu) = -m''n$$

and then, according to Equation (31)

$$(35) \quad I_{(-m''n)n} = -I_{(-m''n)m}.$$

However, from Equations (32) and (33), we obtain $\nu = 0$, which means that we are here concerned with the fields generated by the direct current component of the stator current. The direct current component is always present in the center-tapped circuits without transformer (Table I). The rotation number T compared with the rotor per period of the stator current, for a given component, $I_{(-m''n)n}$ is

$$(36) \quad T = \frac{n \cdot m''}{(\nu)} = -1.$$

This result corresponds to the fact that we are concerned ^{with} ~~if~~ the fields produced by the direct current component, which are at rest with respect to the stator.

An interesting comparison is offered here between the center-tapped circuits and the bridge circuit 3. In this bridge circuit, no direct current component appears in the stator current, so that the relationship between the current harmonics and the harmonics of the current distribution given by Equations (32) and (33), is not useable. Nevertheless, in spite of this, the field harmonics of order $(\nu) = 6k$ determined by Equation (34) are not excluded, and this circuit shows similar properties to those of the center-tap circuit with equal pulse number m . In such a comparison, the advantage of the method developed here again comes into play, that is to say, that the ratios can be compared in the machine without having to look into the stator current harmonics.

b) Circuits with $m_G = 1/2m$

In this group belong the bridge circuits 1, 2, and 3 with the direct supply without transformer, and all circuits except diagram 1 in Table I for the indirect supply through transformer.

In the circuits with $m_G = m$, the spatial motion of all waves towards the rotor was equal. With increasing (ν) , only the angle within which the vectors moved in the "electrical space" increased. However, in all cases, one period of the space vector corresponded to a single pulse of the voltage at the direct current side. However, at $m_G = 1/2m$, it can be established that the vector corresponding to the even order numbers does not periodically describe the same arc on each pulse at the direct current side, but in the course of two successive pulses it describes two arcs q_1 and q_2 (Figure 5), which are rotated by 180° with respect to one another. These two arcs together form one period of the vector under consideration, so that one period corresponds to two pulses. It is clear at first sight, that the average value of the vector in Figure 5 is zero in accordance with (3) which is connected with the fact that the harmonic is not contained in the stator current, whose order (ν) corres-

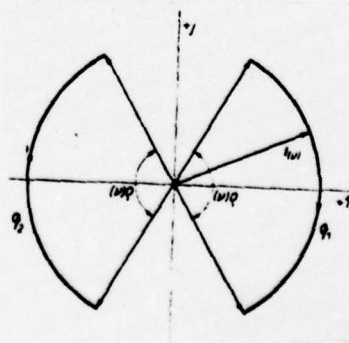


Figure 5. Space vector of the harmonics.

ponds with the order (ν) of the field harmonic under consideration. It can also be easily shown that only components for odd n (both positive and negative) are contained in the series expansion according to Equations (1) and (2). For the series expansion for odd n according to (2), the following applies

$$(37) \quad I_{(\nu)m} = \frac{1}{2\pi} \int_0^{2\pi} i_{(\nu)} e^{-jnx} dx = \frac{1}{\pi} \int_0^{\pi} i_{(\nu)} e^{-jnx} dx = \\ = \frac{1}{\pi} I_{(\nu)m} \int_0^{\pi} e^{-j[(\nu)/m''](2x-\pi)} e^{-jnx} dx = -j \frac{I_{(\nu)m}}{\pi} \frac{m''}{(\nu) + (m''/2)n} \cos \frac{(\nu)}{m''} \pi.$$

In Equation (37) the order of the associated stator current wave also appears again,

$$(38) \quad r = (\nu) + \frac{m''}{2} n$$

where the sign of this expression indicates the direction of rotation of the ν^{th} field wave. Therefore, the following expression applies for (ν):

$$(39) \quad (\nu) = -\frac{m''}{2} n + r,$$

where ν always appears positive and the sign which indicates the direction of rotation appears at the order number (ν).

For the calculation of the effective rotor current distribution, however, it is not necessary to carry out the resolution into individual circular fields. Since the average value of the vector $i_{(\nu)}$ in Figure 5 is equal to zero according to Equation (28), all waves associated with this vector are damped by the rotor and, insofar as the magnetization current is not taken into consideration, the effective rotor load is given directly by the value $I_{(\nu)m}$ of the vector $i_{(\nu)}$.

5. Effect of Commutation

The method derived in the foregoing sections makes possible the relatively simple introduction of the overlap in the commutation into the calculation of the rotor load. We show the calculation procedure in an example which concerns circuit 3 in Table I. In Figure 6 is illustrated the commutation between the lines F and B in

the space of the machine (see circuit 3, Table I) for the case in which the interchange of anodes takes place instantaneously. Anode F completes its work period at point M, and its current is taken over by anode B, so that the vector of the fundamental wave of the stator current distribution jumps from the limiting position $(i_{(1)})'$ into the limiting position $(i_{(1)})''$. The component i_A of the line A, which belongs to the other parallel system, does not change at the instant of commutation. In actuality, the commutation does not take place instantly, but in the course of a definite period, which corresponds to the time angle u'' (based on the cyclic frequency of the generator voltage). The current in the line B increases according to the section of a sinusoidal curve, so that the following equation applies for the current vector of winding B (Figure 6):

$$(40) \quad |i_{(1)B}| = \frac{1}{\sqrt{3}} r_B J_{(1)m},$$

where

$$(41) \quad r_B = \frac{\cos \alpha - \cos(x'/6 + \alpha)}{\cos \alpha - \cos(u'' + \alpha)}$$

In Equations (40) and (41), α designates the lag of the ignition (the control angle in the gating control) of the following anode (here B) with respect to the point of natural commutation, where the anode voltages are equal, and u'' is the overlapping. The variable

$$(42) \quad x' = x - x_0,$$

where x_0 is the value of the integration variable x at the beginning of commutation. In an entirely analogous manner, the following equation applies to the relieved anode F:

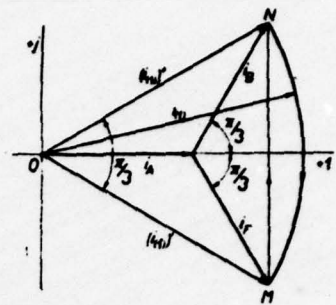


Figure 6. Space vector for 6-pulsed drainage coil circuit.

$$(43) \quad |l_{(1)F}| = \frac{1}{\sqrt{3}} r_F I_{(1)m},$$

where

$$(44) \quad r_F = 1 - r_B = \frac{\cos(x'/6 + \alpha) - \cos(u'' + \alpha)}{\cos \alpha - \cos(u'' + \alpha)}$$

The square of the value of the vector $i_{(1)}$ which is to be inserted in Equation (10), we calculate from the component u which lies in the direction of the vector i_A (Figure 6), and that of the component v perpendicular to this direction. The component u

$$(45) \quad u^2 = \frac{3}{4} I_{(1)m}^2$$

is constant, since the sum of the projections of vectors i_F and i_B on the direction of the vector i_A does not change. For component v ,

$$(46) \quad v = \frac{1}{2} I_{(1)m} (r_B - r_F) = \frac{1}{2} I_{(1)m} \frac{\cos \alpha + \cos(u'' + \alpha) - 2 \cos(x'/6 + \alpha)}{\cos \alpha - \cos(u'' + \alpha)}.$$

If we add the squares of the components u and v , we obtain

$$(47) \quad |l_{(1)}|^2 = u^2 + v^2 = I_{(1)m}^2 \left\{ \frac{\cos^2 \alpha + \cos^2(u'' + \alpha) - \cos \alpha \cos(u'' + \alpha)}{[\cos \alpha - \cos(u'' + \alpha)]^2} + \right. \\ \left. - \frac{\cos \alpha + \cos(u'' + \alpha)}{[\cos \alpha - \cos(u'' + \alpha)]^2} \cos(x'/6 + \alpha) + \frac{1}{[\cos \alpha - \cos(u'' + \alpha)]^2} \cos^2(x'/6 + \alpha) \right\}.$$

according to (10),

$$(48) \quad I_{(1)}^2 = \frac{1}{2\pi} \int_0^{2\pi} |l_{(1)}|^2 dx = \frac{1}{2\pi} \left(\int_0^{6u''} |l_{(1)}|^2 dx + \int_{6u''}^{2\pi} I_{(1)m}^2 dx \right).$$

The first integral is determined with the help of Equation (47) and we obtain (here $x' \equiv x$)

$$(49) \quad \int_0^{6u''} |l_{(1)}|^2 dx = I_{(1)m}^2 (6u'' - 6N),$$

where

$$(50) \quad N = \frac{1}{[\cos \alpha - \cos(u'' + \alpha)]^2} \left\{ \frac{1}{4} [\sin 2(u'' + \alpha) - \sin 2\alpha] + \right. \\ \left. + \sin u'' - \left[\frac{1}{2} + \cos \alpha \cos(u'' + \alpha) \right] u'' \right\}$$

so that

$$(51) \quad I_{(1)}^2 = \frac{1}{2\pi} \int_0^{2\pi} |l_{(1)}|^2 dx = I_{(1)m}^2 \left[1 - \frac{3}{\pi} N \right].$$

By the integration according to Equation (3), we were able to convince ourselves that the average value of the vector $i_{(1)}$ depends little on the commutation up to $u'' = 25^\circ$, so that for small overlaps u'' in accordance with (11) and (12), we can write:

$$(52) \quad \Lambda_{(1)k} = \frac{I_{(1)w}}{I_{(1)0}} = \sqrt{\left[\frac{I_{(1)}^2}{I_{(1)0}^2} - 1\right]} = \sqrt{\left[\left(\frac{\pi}{3}\right)^2 - 1 - \frac{\pi}{3}N\right]}.$$

Equation (52) differs from Equation (19) for $m'' = 6$ only in the term $1/3 \pi N$, which represents the reduction of the effective current load as a result of commutation. In the calculation of N according to Equation (50), the tables of trigonometric functions with more than 5 places are to be used.

Equation (52) is applicable for not too large an angle u'' (up to $u'' = 25^\circ$), to the extent that the commutation does not influence the fundamental wave of the stator current. In Figure 7 is shown the curve of $\Lambda_{(1)k}$ as a function of u'' . The first curve applies to zero-valued control angle α and the other for $\alpha = 10^\circ \div 70^\circ$, since here the value of the control angle affects the curve only slightly.

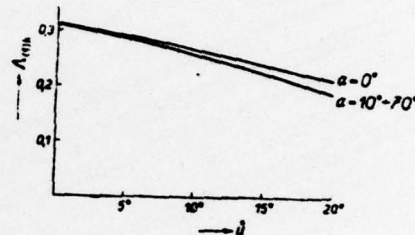


Figure 7. Effect of overlapping

6. Effect of Current Displacement

In the preceding sections, we have derived the value $\Lambda_{(1)}$, which represents the relative value of the fundamental wave of the additional rotor current distribution and which can be compared with the opposing components in unsymmetrical load. However, it is necessary in the comparison to take into account the different rotor impedance which changes with frequency. For the equal-sized equivalent opposing component (which causes the same additional rotor losses), therefore, the following approximation applies:

$$(53) \quad i_A = \frac{I_A}{I_d} = \Lambda_{(1)} \sqrt{\frac{R_f}{R_{100}}} = \Lambda_{(1)} k_f,$$

where R_{100} signifies the rotor resistance at a current frequency of $f_1 = 100$ Hz and R_f indicates the rotor resistance at the frequency of the strongest wave $f_1 = m''f_G$. The factor k_f which considers the current displacement, is calculated either for the entire rotor or for the most sensitive position, where the rotor is most highly threatened (e.g. the end point of the full-drum rotor etc.). It can reach the value

$$(54) \quad k_{fm} = \sqrt{\frac{m''}{2}}.$$

In the exact calculation, and particularly in machines with massive rotors (turbo-generators), however, it is necessary to calculate the corresponding equivalent circuit for the damping winding as well as for the rotor iron, and thereby to determine exactly the growth of the rotor impedance with frequency. In this way, also, a different rotor impedance can be taken into consideration for each component wave of the rotor current.

7. The Distribution of the Current Load on the Rotor Periphery

In the preceding sections, we calculated the effective rotor current distribution and compared it with the effect of the counter-acting components without examining further the distribution at the rotor periphery, which is by no means uniform. If we limit our considerations here to the fundamental wave of the air gap field, we can estimate according to Figure 4, where the damping winding is most heavily loaded. The loading of the rotor is determined by the alternating component $i_{(1)w}$, which is to be calculated as the difference between the vector $i_{(1)o}$ and the total current wave $i_{(1)}$, and which does not rotate with the rotor. The component

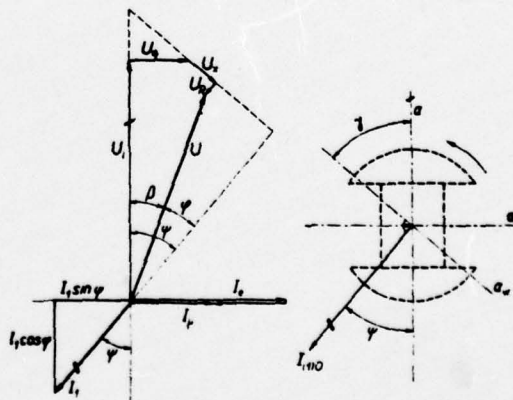


Figure 8. Spatial position of the rotor load

$i_{(1)w}$ represents the momentary maximum of the current wave by its position in the machine space. From the diagram in Figure 4, it results that the current wave $i_{(1)w}$ reaches its largest value in the direction perpendicular to the vector $i_{(1)o}$, whereas its component agreeing with vector $i_{(1)o}$ is only small.²⁾ Therefore, the greatest current load of the rotor is to be expected in the axis perpendicular to the space vector of the fundamental wave of the stator current distribution. The current distribution given by the vector $i_{(1)w}$ has the character of an alternating field, since it acts only in one axis, and so its amplitude is the square root of 2 as large as the ~~single~~ ^{single} rotating field which has the same effective value. This, therefore, means that, insofar as the rotor and the damping winding are fully symmetrical, the losses per unit of rotor surface are twice as great as for a uniform distribution, which for example, occurs with the counteracting components. The position of this maximum current load on the rotor periphery can be determined on the basis of the usual vector diagram of the synchronous machine, as is illustrated in Figure 8 for a side pole machine. (The same applies to turbogenerators.) As shown in Figure 8, the greatest loading of the damping winding is to be expected in the axis A_w (Figure 8b), which with the rotor axis a , includes the angle:

$$(55) \quad \gamma = 90^\circ - \psi = 90^\circ - \beta - \varphi$$

Besides the fact that the pulsating wave signifies the concentration of the losses in one axis, the currents in the rotor are also affected by the asymmetry of the damping winding, so that in an exact calculation, the vector $i_{(1)w}$ is to be resolved into a longitudinal and a transverse component, and the currents in the damping winding are to be determined independently for each component. For the

2) It is even more apparent, if we resolve the vector $i_{(1)}$ into circular fields. The pair of components with equal ~~line~~ $|n|$ ~~line~~ form elliptical rotating fields, whose longer axis is perpendicular to the vector $i_{(1)o}$ and is nm times as long as the shorter axis.

approximate comparison with the counteracting component, it suffices to estimate that in machines with a small synchronous reactance (side pole machines), which are loaded with an uncontrolled rectifier (the phase angle φ is only given by the overlapping u), larger values of γ are to be expected, whereas in turbogenerators and particularly the ignition lag, the values of γ turn out to be smaller. The angle γ becomes all the larger, the greater is the rated output in comparison with the output of the fundamental wave (because of the additional losses), since in this way the relative value of the synchronous reactance becomes smaller. Therefore, in a machine loaded with a rectifier, angles γ larger than 45° (to 60°) cannot be excluded, so that the transverse component of the current load can be larger than the longitudinal component. It is known that the damping of the transverse component of the current distribution is connected with greater overload of the outer bars of the damping winding, if this is not carried out symmetrically. It is, therefore, necessary in a precise calculation to devote appropriate attention to the overloading of the rim bars, specifically at the starting edge, where the results of the longitudinal and transverse components add together. The overloading of the rim bars caused by the transverse components of the current distribution can be limited, if the field coil is terminated through a small impedance, so that the field coil supplements the damping winding in the transverse axis or when short-circuiting windings are on the pole sides.

In turbogenerators, where the damping winding is generally accommodated in the same grooves as the field coil, in comparison with the counteracting component of equal size, only the local $\sqrt{2}$ -fold increase of the current distribution is to be reckoned with. This increase of the current load is imparted by the alternating character of the current distribution wave.

8. Complicated Circuits

In this section it is shown that the process developed for the calculation of rotor losses is suitable for the most complicated cases. In Figure 9 is illustrated the circuit which is used

for the energizing of large turbo-generators. It is a case of a 6-phase auxiliary generator which supplies the exciter circuit of the principal machine through rectifiers. The basic circuit of the auxiliary generator corresponds to the center-tapped circuit 3 in Table I, which was previously mentioned in Section 5. Each line of the stator winding, however, has two rectifiers G and G', of which the first rectifier ^{provides} protects the normal excitation and the other ^{provides} protects the step excitation. In the case of a short-circuit, the rectifier G' must be completely prepared to operate, so that it is necessary to load it even in continuous operation with short current pulses, which last about 1/5th of the operating period of the rectifier G. Upon ignition of the rectifier G', the associated rectifier G becomes extinguished, and the current flows through the entire winding line. For the machine, this means a sudden climb of the armature reaction, as if the stator current had

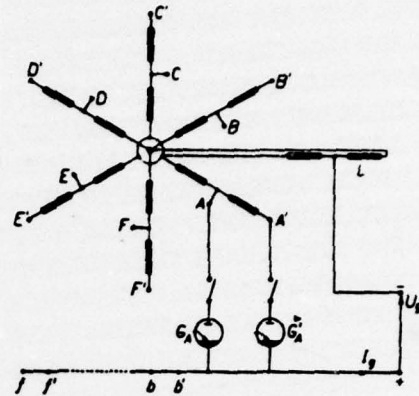


Figure 9. 6-pulse drainage coil circuit for two voltages.

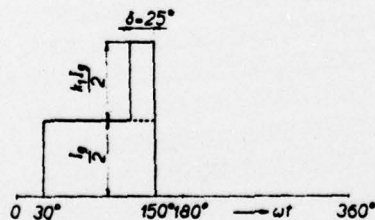


Figure 10. Equivalent flow of the stator current.

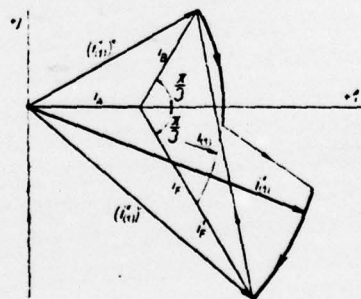


Figure 11. Space vector of the fundamental wave.

grown. In Figure 10 is illustrated the shape of such an equivalent current for the case in which the ratio of the effective number of turns of the two line sections $k_{(1)} = 1$, and the duration of burning of the rectifier G' corresponds to the time angle $\delta = 25^\circ$.

The additional losses caused by the fundamental wave of the air-gap field in the rotor, are again calculated from the shape of the space vector $i_{(1)}''$, which is illustrated in Figure 11. Figure 11 differs from Figure 6 in the additional vector i_F^1 which corresponds to the effect of the winding for step excitation.

For the average value of the vector $i_{(1)}''$, we obtain from Equation (3)

$$(56) \quad I_{(1)0}'' = \frac{1}{2\pi} \int_0^{2\pi} I_{(1)}'' dx = \frac{1}{2\pi} \int_0^{2\pi-6\delta} I_{(1)} dx + \frac{1}{2\pi} \int_{2\pi-6\delta}^{2\pi} \left(I_{(1)} + \frac{k_{(1)}}{\sqrt{3}} I_{(1)m} e^{-j(\pi/6)} \right) dx =$$

$$= I_{(1)0} + \frac{k_{(1)}}{2\pi\sqrt{3}} \int_{2\pi-6\delta}^{2\pi} I_{(1)m} e^{-j(\pi/6)} dx = I_{(1)m} \left[\frac{3}{\pi} + \frac{2\sqrt{3}}{\pi} k_{(1)} \sin \frac{\delta}{2} e^{-j(\pi/3-\delta/2)} \right].$$

From this, it follows that

$$(57) \quad |I_{(1)0}''|^2 = I_{(1)m}^2 \left| \frac{3}{\pi} + \frac{2\sqrt{3}}{\pi} k_{(1)} \sin \frac{\delta}{2} e^{-j(\pi/3-\delta/2)} \right|^2 =$$

$$= I_{(1)m}^2 \left[\frac{9}{\pi^2} + \frac{12}{\pi^2} k_{(1)}^2 \sin^2 \frac{\delta}{2} + \frac{12\sqrt{3}}{\pi^2} k_{(1)} \sin \frac{\delta}{2} \cos(\pi/3 - \delta/2) \right].$$

The effective value of the vector $i_{(1)}''$ is given in accordance with (10) as

$$(58) \quad I_{(1)}''^2 = \frac{1}{2\pi} \int_0^{2\pi} |I_{(1)}''|^2 dx = \frac{1}{2\pi} I_{(1)m}^2 \int_0^{2\pi-2\delta} dx +$$

$$+ \frac{1}{2\pi} I_{(1)m}^2 \int_{2\pi-6\delta}^{2\pi} \left| 1 + \frac{k_{(1)}}{\sqrt{3}} e^{-j\pi/6} \right|^2 dx = I_{(1)m}^2 \frac{1}{2\pi} \left\{ 2\pi - 6\delta + \left| 1 + \frac{k_{(1)}}{\sqrt{3}} e^{-j\pi/6} \right|^2 6\delta \right\},$$

so that after certain transformation, we obtain

$$(59) \quad I_{(1)}''^2 = I_{(1)m}^2 [1 + (3k_{(1)} + k_{(1)}^2) \delta/\pi].$$

For the relative values of the equivalent circular field, in accordance with Equations (11), (57), and (59), the following equation applies:

$$(60) \quad A_{(1)} = \frac{I_{(1)w}''}{I_{(1)0}''} = \sqrt{\frac{\pi[\pi + (3k_{(1)} + k_{(1)}^2) \delta]}{9 + 12k_{(1)}^2 \sin^2 \delta/2 + 12\sqrt{3} k_{(1)} \sin \delta/2 \cos(\pi/3 - \delta/2)} - 1}.$$

Of great significance also, is the ratio of the effective amplitude of the alternating component $i_{(1)w}''$ to the alternating wave $i_{(1)0}$ of the winding, for the basic excitation

(61)

$$A_{(1)}' = \frac{I_{(1)w}''}{|I_{(1)0}|} = A_{(1)} \frac{|I_{(1)0}|}{|I_{(1)0}|} = \sqrt{\left(\frac{I_{(1)}'^2 - |I_{(1)0}|^2}{|I_{(1)0}|^2}\right)} = \frac{1}{3} \sqrt{\{\pi[\pi + (3k_{(1)} + k_{(1)}^2) \delta] - [9 + 12k_{(1)}^2 \sin^2 \delta/2 + 12\sqrt{3} k_{(1)} \sin \delta/2 \cos(\pi/3 - \delta/2)]\}}$$

In Table IV are the values of $\Lambda_{(1)}$ and $\Lambda_{(1)}'$ for $k_{(1)} = 1; 1.2$ and for a burning time of the high voltage rectifier $\delta = 25^\circ; 30^\circ; 35^\circ$. Figure 12 shows the dependence of the Λ' factor on $k_{(1)}$ for $\delta = 25^\circ$ and $\delta = 35^\circ$. From comparison of the calculated values of $\Lambda_{(1)}$ and $\Lambda_{(1)}'$ for the value $\Lambda_{(1)} = 0.311$ indicated in Table I, it results that the current pulses in the high voltage winding increased the additional losses in the machine almost two-fold, so that this circuit is very unfavorable from the standpoint of the machine. It is apparent from Figure 12, that the burning time of the high voltage rectifier influences the losses only slightly.

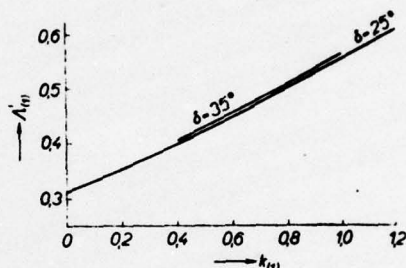


Figure 12. Effect of the number of turns of the high voltage winding.

Table IV
Current Load (1)

$k_{(1)}$		$\delta = 25^\circ$	$\delta = 30^\circ$	$\delta = 35^\circ$
1.0	$\Lambda_{(1)}$	0,467	0,457	0,441
1.0	$\Lambda_{(1)}'$	0,553	0,561	0,562
1.2	$\Lambda_{(1)}$	0,496	0,483	0,469
1.2	$\Lambda_{(1)}'$	0,608	0,616	0,625

9. Summary

In the present paper is developed a new method for calculation of the additional losses which occur in the rotor of the synchronous machine loaded by rectifiers, as a result of the pulse-shaped curve of the stator currents. This procedure is based on the direct calculation of the current load of the damping winding from the shape of the space vector of the current distribution, without necessity of expanding the stator currents into Fourier series and adding the component losses of the individual current components. The influence of the additional fields is compared with the effect of the counteracting component ⁱⁿ of the unsymmetrical loading of the machine. This simple calculation procedure makes possible the evaluation of the various rectifier circuits from the standpoint of the machine, and to compare them, and to establish a number of interesting generally valid relationships, of which the following merit particular mention:

a) The greatest additional rotor losses are produced by the fundamental wave of the air gap field, which move forward in jumps, wherein the number of jumps corresponds to the number of pulses of the rectified voltage. Thus, the number of pulses of the direct current side is decisive for the rotor losses, independently of the number of winding lines or rectifiers.

b) The values $\Lambda_{(1)}$ are listed in Tables I and II for comparison of the particular types of circuits; these values represent the ratio of the effective rotor load to the working wave, and can be compared with the permissible relative sizes of the counteracting components in the unsymmetrical load (skew load). From the values of $\Lambda_{(1)}$, it results that the additional current load of the rotor assumes significantly larger values than is indicated in the literature (10) and than is permitted in unsymmetrical loading.

c) The space harmonics of the stator distribution contribute comparatively little to the rotor losses, and their effect can be established in the same way as in the case of the fundamental wave.

d) The calculation process developed, also makes it possible to take into consideration the overlapping in commutation. It slightly reduces the additional losses (see Figure 7).

e) The additional current load is not uniformly distributed at the rotor periphery (as in the case of the counter-acting component), but is concentrated on one axis, which leads to a great overload of the rim bars of the damping winding at the starting edge of the pole piece.

f) By insertion of a transformer between the rectifier and the generator, the additional rotor losses cannot significantly be reduced, since the fundamental wave of the stator current distribution which causes most of the additional losses, is not influenced in this way. Connected with this is the fact that the stator current waves determined by Equation 23, which are connected with the fundamental wave of the air gap field, cannot be eliminated by insertion of the transformer.

g) The circuit in Figure 9 with current pulses in the high voltage rectifiers, shows large additional rotor losses which can be compared in the unsymmetrical loading, with those from the counteracting component, at 50%.

Character Symbols

U_g	Direct current voltage
I_g	Direct current
U	Fundamental wave of the generator voltage
U_l	Longitudinal component of the generator voltage
U_q	Transverse component of the generator voltage
I	Effective value of the generator current
i_l	Fundamental wave of the generator current
$i_{(1)}$	Space vector of the fundamental wave of the stator current distribution
$I_{(1)m}$	The maximum value of the vector $i_{(1)}$
$I_{(1)o}$	Average value of the vector $i_{(1)}$
$I_{(1)n}$	Components of the vector $i_{(1)}$
$i_{(1)w}$	Alternating component of the vector $i_{(1)}$
$I_{(1)w}$	Effective value of the alternating component $i_{(1)w}$
$I_{(1)}$	Effective value of the vector $i_{(1)}$
$i_{(\nu)}$	Vector of the $(\nu)^{th}$ space wave
$S_{(\nu)}$	Effective number of rods

f	Frequency of the generator voltage
f_1	Frequency of the strongest rotor current wave
m_G	Number of phases of the generator
m''	Number of pulses of the rectification (number of ignitions per period of the stator current)
$k_{(1)}$	Effective turns ratio
ω	Angular velocity
u''	Duration of overlap
α	Control angle
x	Solid angle
δ	Burning time of the high voltage rectifier
$\xi_{(n)}$	Winding factor of the n^{th} harmonic
ν	Order of the current harmonic
(ν)	Order of the space harmonic
n	Order of the vector component
$\Lambda_{(1)}$	Relative size of the current load of the fundamental wave
$\Lambda'_{(1)}$	Relative size $\Lambda_{(1)}$ with consideration of the high voltage winding
Λ_{1-1}	Relative value $\Lambda_{(1)}$ originating from the two strongest waves
$\Lambda_{(1)k}$	Relative value $\Lambda_{(1)}$ with consideration of commutation.

References

- [1] Heller B.: Vliv usměrňovačů na provoz alternátorů a transformátorů (Einfluss der Gleichrichter auf den Betrieb von Generatoren und Transformatoren.) Elektrotechnický obzor 40 (1951), S. 173.
- [2] Bašta J.: Teorie elektrických strojů (Theorie der elektrischen Maschinen). Prag, NČSAV, 1957.
- [3] Kučera J.: Harmonische Flächenanalyse der magnetomotorischen Kräfte in der Mehrphasenwicklung. E. u. M. (1954), S. 231.
- [4] Ibl J.: Průmyslová elektronika II (Industrielle Elektronik II), Prag, SNTL, 1955.
- [5] Sequens H.: Die Wicklungen elektrischer Maschinen, Wien, Springer, 1950.
- [6] Štěpina J.: Die Einzelwellen der Felderregerkurve bei unsymmetrischen Asynchronmaschinen. Archiv für Elektrotechnik 43 (1958), H. 6, S. 384—402.
- [7] Štěpina J.: Die physikalische Bedeutung der symmetrischen Komponenten der Momentanwerte und ihre Verallgemeinerung. Acta Technica (1962), H. 5, S. 451.
- [8] „Hütte“ des Ingenieurs Taschenbuch IVA, Elektrotechnik, Ernst und Sohn, Berlin 1957.
- [9] Dällenbach W. und Gerecke E.: Die Strom- und Spannungsverhältnisse der Grossgleichrichter. A. f. E. XIV (1924), S. 171—220.
- [10] Štrafun Ju. N.: Puti vozmožnogo razvitiya avtomatičeski regulirujemych sistem vozbuždenija turbogeneratorov (Die Entwicklungsmöglichkeiten der automatisch geregelten Erregung von grossen Turbogeneratoren). Električestvo (1959), H. 12, S. 10.
- [11] Krämer W.: Stationäre Stromverteilung im Dämpferkäfig von Schenkelpolmaschinen. ETZ-A83 (1962), H. 5, S. 111.

DISTRIBUTION LIST

DISTRIBUTION DIRECT TO RECIPIENT

ORGANIZATION	MICROFICHE	ORGANIZATION	MICROFICHE
A205 DMATC	1	E053 AF/INAKA	1
A210 DMAAC	2	E017 AF/ RDXTR-W	1
B344 DIA/RDS-3C	8	E404 AEDC	1
C043 USAMIA	1	E408 AFWL	1
C509 BALLISTIC RES LABS	1	E410 ADTC	1
C510 AIR MOBILITY R&D	1	E413 ESD	2
LAB/FIO		FTD	
C513 PICATINNY ARSENAL	1	CCN	1
C535 AVIATION SYS COMD	1	TQIS	3
		NIA/PHS	1
C591 FSTC	5	NICD	2
C619 MIA REDSTONE	1		
D008 NISC	1		
H300 USAICE (USAREUR)	1		
P005 ERDA	1		
P055 CIA/CRS/ADD/SD	1		
NAVORDSTA (50L)	1		
NASA/KSI	1		
AFIT/LD	1		